ACS APPLIED MATERIALS & INTERFACES

RESEARCH ARTICLE

www.acsami.org

Antibacterial Performance of Polydopamine-Modified Polymer Surfaces Containing Passive and Active Components

Tadas S. Sileika,[†,‡] Hyung-Do Kim,[†,‡] Piotr Maniak,[†] and Phillip B. Messersmith[*,†,§,⊥,#,||,△]

[†]Biomedical Engineering Department [§]Materials Science and Engineering Department [⊥]Chemical and Biological Engineering Department [#]Chemistry of Life Processes Institute [||]Institute for Bionanotechnology in Medicine [△]Robert H. Lurie Comprehensive Cancer Center Northwestern University, Evanston, Illinois 60208, United States

Supporting Information

ABSTRACT:

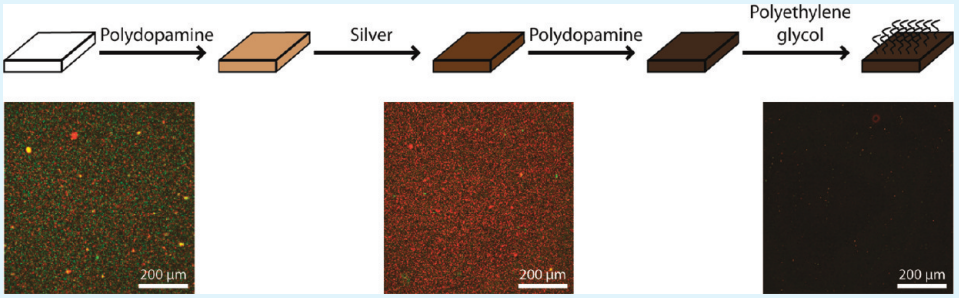

A growing number of device-related nosocomial infections, elevated hospitalization costs, and patient morbidity necessitate the development of novel antibacterial strategies for clinical devices. We have previously demonstrated a simple, aqueous polydopamine dip-coating method to functionalize surfaces for a wide variety of uses. Here, we extend this strategy with the goal of imparting antifouling and antimicrobial properties to substrates, exploiting the ability of polydopamine to immobilize polymers and induce metal nanoparticle formation. Polydopamine was deposited as a thin adherent film of 4 nm thickness from alkaline aqueous solution onto polycarbonate substrates, followed by grafting of antifouling polymer polyethylene glycol and in situ deposition of silver nanoparticles onto the polydopamine coated polycarbonate substrates. Elemental and morphological surface analyses confirmed successful grafting of polyethylene glycol brushes onto polydopamine-coated substrates, as well as spontaneous silver nanoparticle formation for polydopamine-coated substrates incubated in silver-nitrate solutions. Sustained silver release was observed over at least 7 days from silver-coated substrates, and the release kinetics could be modulated via additional polydopamine overlayers. In vitro functional assays employing gram negative and positive strains demonstrated dual fouling resistance and antibacterial properties of the coatings due to the fouling resistance of grafted polyethylene glycol and antibacterial effect of silver, respectively. Polycarbonate substrates coated only with silver using a method similar to existing commercial coatings provided an antibacterial effect but failed to inhibit bacterial attachment. Taking into account the previously demonstrated substrate versatility of polydopamine coatings, our findings suggest that this strategy could be implemented on a variety of substrate materials to simultaneously improve antifouling and antimicrobial performance.

KEYWORDS: antifouling, antimicrobial, antibacterial, infection, silver, nanoparticle, coating, dopamine, polymer

INTRODUCTION

Hospital-acquired infections have been on the rise in the past decade with staggering numbers.[1,2] 1.7 million hospitalized patients were afflicted by nosocomial infections (NIs) in 2002, of which almost 100 000 cases resulted in fatalities.[1] Almost half of all NIs are device-related, with the greatest percentage of cases consisting of urinary tract (UTI) and central venous catheterization-related infections. Peripheral complications often arise in the form of bloodstream and surgical site infections, as well as pneumonia.[2,3] Combining even moderately invasive procedures with an already compromised immune response of a hospitalized patient provides opportunistic bacteria with optimal conditions for infection.[4−6] To reduce the growing number of NI cases and associated hospitalization costs, it is crucial to develop materials that resist or prevent bacterial attachment, establishment, and proliferation in catheters and other medical devices.

Device-associated infections can progress rapidly as planktonic bacteria first adhere to a medical device surface and ultimately evolve into biofilms.[4] Once in sessile biofilm configuration, bacteria express drastically different phenotypes compared to the planktonic state, marked by decreased metabolic activity and the production of an extracellular polymeric substance (EPS) matrix. The EPS functions in nutrient scavenging as well as shielding against chemical, physiological and environmental

Received: July 26, 2011
Accepted: November 1, 2011
Published: November 01, 2011

factors that could adversely affect the bacteria.[6] Studies have shown that upon biofilm formation, the amount of antibiotic necessary for treatment can be as much as 1500 times greater than for planktonic cells.[7] The infection and treatment outlook is further complicated by fragmentation of biofilms, which can become dislodged by mechanical forces and transported through device tubing to other locations within the urinary tract and cardiovascular system.[2]

Prevention of biofilm formation has therefore been of recent interest to biomaterials researchers, whose efforts have focused on the design of coatings tailored for this purpose.[8,9] With respect to coating strategies we distinguish between passive (antifouling) and active (antimicrobial) strategies. Passive strategies rely on inhibition of bacterial attachment, typically through physical prevention of nonspecific cell attachment by a grafted polymer coating, whereas as active strategies rely on the presence of an antibacterial compound that actively promotes bacterial killing by interfering with biochemical pathways leading to toxic effects.[10−12] Active strategies can be further classified as exerting either off-surface effects, i.e., through elution of antibacterial compounds into the biological milieu, whereupon they target planktonic cells − or on-surface effects via grafting of antibacterial compounds directly onto the surface for targeting of attached cells.[8,13]

A variety of antifouling and antimicrobial coating strategies are actively being explored for preventing medical device-related infections. Some currently marketed devices exhibit antimicrobial behavior through release of an active agent, typically silver.[5] Silver's nonspecific antimicrobial benefits are well-known and have been increasingly investigated in the form of silver-based device coatings.[10,11,14−18] Commercially available coatings containing silver nanoparticles embedded in a polymer matrix have been shown to exhibit active antimicrobial behavior in both in vitro and in vivo studies.[19] Passive antifouling coating strategies have focused on the use of polyethylene glycol (PEG) brushes or other grafted polymer steric barriers to prevent bacterial attachment through steric hindrance.[20−25] Although in vitro studies yielded promising results, in vivo results have been mixed and clinical implementation limited. Approaches that involve both active (antimicrobial) and passive (antifouling) mechanisms as a part of a single unified coating strategy are still uncommon.[26−29]

One challenge for the widespread practical implementation of all types of antibacterial coatings relates to their capacity to be applied to different types of substrate materials via simple and inexpensive precleaning strategies and fabrication methods. Recently, we reported the development of mussel-inspired coatings deposited onto a variety of organic and inorganic surfaces via a simple immersion method.[30] The method relies on surface-initiated polymerization of dopamine, a small molecule analog of the catechol and amine rich proteins of marine mussels.[31,32] Under mild alkaline aqueous conditions and in the presence of oxygen, dopamine polymerizes to form thin adherent films of polydopamine (pDA) on virtually any surface. Moreover, exposed reactive groups of the pDA coatings enable further functionalization of the coatings through covalent grafting of polymers and deposition of metal films via reduction of metal ions.[30,33,34]

In this study, we report a novel antibacterial coating strategy that takes advantage of the versatile features of the pDA chemistry to integrate both antimicrobial and antifouling elements into the coating. The strategy utilizes a simple immersion-coating process to deposit pDA onto polycarbonate (PC) substrates. The pDA coating then serves as a "primer", onto which silver nanoparticles and PEG are deposited to confer antibacterial and antifouling characteristics, respectively. The resulting coatings resisted bacterial cell attachment and killed clinically relevant gram negative and gram positive strains. This strategy is simple to implement and can be easily adapted for other substrates.[3,35,36]

MATERIALS AND METHODS

Materials. All test coatings were prepared on square pieces of injection-molded PC (Makrolon 2458; Bayer, Pittsburgh, Pennsylvania) measuring $1.3 \times 1.3 \times 0.3$ cm^3, provided by Baxter Healthcare. Absolute isopropanol, NaCl, and NaOH were purchased from VWR International (West Chester, Pennsylvania). 12-well tissue culture plates were purchased from BD Falcon (Franklin Lakes, New Jersey). Twenty milliliter glass scintillation vials were purchased from Wheaton (Millville, New Jersey). Bicine, dopamine·HCl, $AgNO_3$, sodium-acetate, and N,N,N′, N′-tetramethylethylenediamine (TEMED) were purchased from Sigma (St. Louis, Missouri). Tween 20 was purchased from Fluka (Milwaukee, Wisconsin). Methoxy-poly(ethylene glycol)-thiol (mPEG-SH; 5000 MW; lot # 116−164) was purchased from Laysan Bio (Arab, Alabama). KCl was purchased from Fischer BioReagents (Fair Lawn, New Jersey). Nitric acid was purchased from Aldrich Chemistry (St. Louis, Missouri). Internal standards for ICP (^{45}Sc, ^{159}Tb, ^{89}Y, ^{115}In, and ^{209} Bi) were purchased from Peak Performance, CPI International (Santa Rosa, California). Biofilm-producing strains of *Escherichia coli* (ATCC 35218), *Staphylococcus epidermidis* (RP62A), and *Pseudomonas aeruginosa* (ATCC 27853) were purchased from ATCC (Manassas, Virginia). Difco Luria−Bertani (LB) broth and Bacto Tryptic-Soy broth were purchased from BD Diagnostic Systems (Sparks, Maryland). Syto-9/Propidium-Iodide BacLight Bacterial Viability Kit and BacLight Mounting Oil were purchased from Invitrogen (Eugene, Oregon).

Surface Modification. PC substrates were treated as illustrated in Figure 1 and described in detail below. Prior to surface modification, as-received PC substrates were immersed in isopropanol, sonicated for 10 min, rinsed with deionized (DI) water 3 times, and air-dried for 24 h. Modification of PC substrates was performed in triplicate in 20 mL glass scintillation vials. Unless otherwise indicated, all modifications were performed at room temperature on a temperature-controlled orbital shaker (KS 4000i Control; IKA, Wilmington, North Carolina) rotating at 70 rpm. Preliminary optimization studies were performed to identify the conditions used for polydopamine, silver deposition, and PEG grafting, and details can be found in the Supporting Information (Figures S1 and S2). For protocols involving multiple incubation steps, substrates were rinsed with DI water and gently dried with nitrogen gas between steps and after the completion of the protocol. The volumes of solutions reported below are per vial.

Polycarbonate (PC). PC control substrates were incubated in 10 mL of 10 mM bicine buffer (pH 8.5) for 18 h at room temperature.

Directly Deposited Silver (DDS). DDS modified PC substrates were prepared according to the following protocol. A reaction mixture of 1.1 mM Tween 20, 12 mM $AgNO_3$, and 4.1 mM sodium-acetate was prepared in a beaker in 1000 g of DI water. The solution was heated to 67 °C and 43 mM of TEMED was added to initiate the reaction. PC samples were suspended on a custom holder assembly and submerged into the reaction solution, stirring at roughly 60 rpm. The reaction proceeded for 6 h, with 100 mL of water added in 50 mL aliquots to counteract evaporative losses.

Polydopamine (pDA). PC substrates were immediately submerged in 10 mL of a freshly prepared 0.1 mg/mL solution of dopamine·HCl in 10 mM bicine buffer (pH 8.5) for 18 h at room temperature.

Polyethylene Glycol (PEG). pDA substrates were covered with 5 mL of 1 mM mPEG-SH in 0.6 M KCl and 10 mM bicine, pH 8.5, and incubated for 6 h at 55 °C.

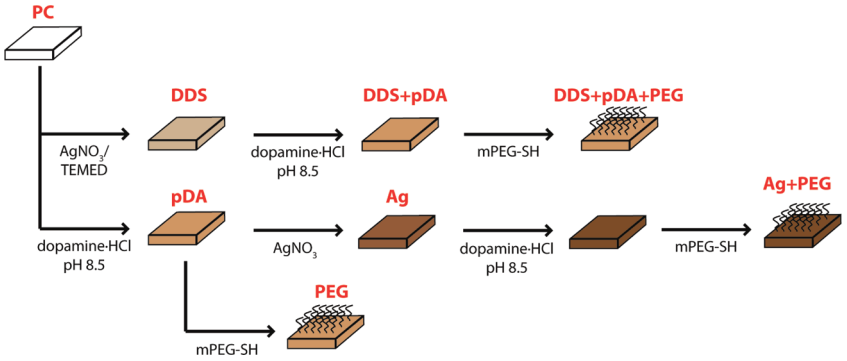

Figure 1. Preparation protocol for directly deposited silver (DDS) and polydopamine-mediated antibacterial coatings (pDA, PEG, Ag, Ag+PEG, DDS+pDA, DDS+pDA+PEG). All substrates were prepared on 1.3 × 1.3 × 0.3 cm^3 samples of polycarbonate (PC).

Silver (Ag). pDA substrates were incubated in 10 mL of 50 mM $AgNO_3$ for 24 h at room temperature.

Silver with Polyethylene Glycol (Ag+PEG). Ag substrates were incubated in 10 mL of 0.1 mg/mL dopamine·HCl solution for 4 h at room temperature, followed by incubation in 5 mL of 1 mM mPEG-SH in cloud point buffer for 6 h at 55 °C.

DDS with Polydopamine (DDS + pDA). DDS substrates were submerged in 10 mL of a freshly prepared 0.1 mg/mL solution of dopamine·HCl in 10 mM bicine buffer (pH 8.5) for 18 h at room temperature.

DDS with Polyethylene Glycol (DDS + pDA + PEG). DDS substrates were incubated in 10 mL of 0.1 mg/mL dopamine·HCl solution for 4 h at room temperature, followed by incubation in 5 mL of 1 mM mPEG-SH in cloud point buffer for 6 h at 55 °C.

Substrate Characterization. X-ray photoelectron spectroscopy (XPS) (Omicron ESCA Probe; Omicron, Taunusstein, Germany) was utilized to characterize the chemical composition of substrates. Substrates were left in the introduction chamber of the XPS apparatus to outgas overnight prior to analysis. The X-ray source operated at 300 W with a spot size of 1.5 mm and a constant sample deflection angle of 45°. An electron gun was used to minimize surface charging effects, operating with a beam current of 0.008 mA at 12.5 eV. Analysis chamber pressure was maintained below 3×10^{-9} Pa during operation. Spectrum survey scans were performed between 0 and 1100 eV electron binding energies. High-resolution spectra of the C_{1s} region were obtained by averaging 3 separate sweeps between 277.5 and 292.5 eV.

Static contact angle measurements were performed by a sessile drop method using a goniometer (model 100−00−115, Ramé-Hart Instruments, Netcong, New Jersey) coupled to an automated pipetting system (Ramé-Hart Instruments, Netcong, New Jersey). Contact angles were measured using 10 μL drops of water three times on $N = 3$ substrates.

Atomic force microscopy (AFM) (MFP-3D; Asylum Research, Santa Barbara, California) was used to assess morphological characteristics of coated substrates. High-aspect-ratio probes (Super Sharp Silicon − NCHR; Nanosensors, Neuchatel, Switzerland) were tuned to respective resonant frequencies using driving amplitude of 1.8 V for AC tapping-mode analysis. Scanning parameters were set as follows: 5 × 5 μm scan size, 512 × 512 pixel raster, 1.44 V driving amplitude, 400 mV set-point, integral gain of 3.0, proportional gain of 0.3, and input gain of 12 dB.

Scanning electron microscopy (SEM) (S-4800 FE-SEM; Hitachi, Schaumburg, Illinois) was used in conjunction with energy-dispersive X-ray spectroscopy (EDS) (Prism 2000; Princeton Gamma Tech Instruments, Princeton, New Jersey). SEM imaging was performed with the following parameters: 15.0 kV accelerating voltage, 10 μA beam current, 3 mm stage distance, and 22K magnification. Polydopamine coating thickness was determined by imaging pDA substrates after incubation in 1 mM $AgNO_3$ solution for 2 h, effectively "staining" the polydopamine layer without formation of silver nanoparticles (see the Supporting Information, Figure S3). The silver-stained pDA substrates were fractured and then the fracture surface imaged using 20 kV accelerating voltage, 20 μA beam current, 8 mm stage distance, and 800K magnification. The presence of nanoparticles on Ag substrates was confirmed through EDS and UV−vis analysis. EDS line scans were performed on 3 adjacent nanoparticles for 10 min using 7 kV accelerating voltage and 20 μA beam current, with characteristic electron counts obtained for carbon (La1) and silver (Ka1). UV−vis spectral scans of modified substrate samples were performed from 800 to 300 nm with 1 nm step size.

Particle count, surface area and volume measurements were obtained by analysis of AFM images using ImageJ software (Version 1.42q, Wayne Rasband, National Institutes of Health, USA). Silver nanoparticle diameter distribution was determined through image analysis of 3 SEM scans of Ag substrate samples.

Silver Release Determination. Silver release was quantified for up to 10 days by inductively coupled plasma mass spectroscopy (ICP-MS) (X Series 2; Thermo-Fisher Scientific, Pittsburgh, Pennsylvania). Sample substrates were individually placed into 20 mL scintillation vials, immersed in 5 mL of 0.85% NaCl solution (saline), and incubated at 37 °C without agitation. Substrates were removed daily and placed into new vials containing 5 mL of fresh saline solution to simulate sink conditions, with 3 samples prepared per experimental group. For ICP-MS analysis, 800 μL of solution from each vial was combined with 160 mg of 70% nitric acid and 40 μL of 1 ppm internal standard, and then diluted to 8 mL with nanopure water. The ICP-MS parameters were fixed at 25 ms uptake time for the sample and 40 ms rinse time using 3% nitric acid. Silver release was quantified by measuring the concentration of ^{107}Ag in each 8 mL sample. The total mass of silver released over 10 days was determined by summing the measured mass of ^{107}Ag from the daily samples, with sample averages obtained from 3 separate ICP-MS sweeps.

Bacterial Attachment and Death Assays. Antifouling and antimicrobial behavior of the generated surfaces were evaluated using three bacterial strains. *E.coli* was cultured in LB broth and *S.epidermidis* and *P.aeruginosa* were cultured in Tryptic-Soy broth. After an overnight culture at 37 °C, respective CFU counts were determined from measured absorbances at 600 nm wavelength using previously established standard curves. Cells were centrifuged at 10 000 rpm at 4 °C (5804 R Centrifuge; Eppendorf, Hamburg, Germany) and the pellets resuspended in sterile saline solution.

For the bacterial attachment assay, sample substrates were placed into wells of a 12-well tissue culture plate and covered with 2 mL of 1×10^8 CFU/mL of the desired strain. The samples were kept in an incubator for 24 h at 37 °C, washed with saline, stained with a live/dead stain, washed 3 more times with saline, and mounted on glass microscope slides using mounting medium for fluorescence imaging.

For the death assay, 20 μL of 2.5 $\times$ 10^9 CFU/mL of each strain, suspended in saline and premixed with a live/dead stain, were placed onto glass microscope slides, covered with a sample substrate, and the edges sealed using a heated mixture of VALAP (1:1:1 ratio of Vaseline, lanolin and paraffin). Samples were incubated at 37 °C for 24 h prior to imaging.

Fluorescence imaging was performed using a Leica microscope (Leica DM IRB; Leica Microsystems, Bannockburn, Illinois). Three images per substrate and N = 3 substrates were collected. ImageJ was used to subtract background, manually set thresholds, and calculate total percentage of area covered for the attachment assay, and fraction of dead cells for the death assay. Values were normalized to PC controls for both assay types. Statistical significance was determined via one-way ANOVA and the Bonferroni post-test.

RESULTS AND DISCUSSION

Polydopamine-Coated Substrates Enable the Dual Incorporation of PEG and Silver via a Simple Dip-Coating Procedure. We hypothesized that the previously demonstrated versatile chemistry of polydopamine would enable the modification of medically relevant substrates with both passive and active agents for the prevention of microbial biofilms. For silver deposition, we took advantage of the inherent reductive capacity of polydopamine films, which give rise to direct metal film deposition upon exposure to noble metal salt solutions.[30,37] This feature is likely due to redox reactions between residual catechols in the polydopamine film and Ag^+ ions, forming Ag^0 at the solid−liquid interface. On the other hand, quinone functional groups in mussel mimetic polymers and polydopamine coatings offer convenient sites for covalent grafting of nucleophilic polymers and biomolecules via Michael addition and/or Schiff base reactions.[38,39] Antifouling polymers, such as PEG, terminally functionalized with primary amines and sulfhydryls can be grafted onto polydopamine coatings to confer resistance to biofouling by proteins and cells.[30]

To systematically demonstrate the use of polydopamine in antibacterial applications, we generated several polydopamine based coatings containing silver and grafted PEG (Figure 1) and assessed their antibacterial performance in comparison to unmodified polycarbonate and a directly deposited silver-based coating similar to a commercially available coating. All substrate modification steps involved immersion of substrates at mild temperature in aqueous solvents of either neutral or slightly basic pH, making the method simple, versatile, and cost-effective.

The first step in our coating strategy involved deposition of a uniform polydopamine (pDA) "primer" coating on the polycarbonate substrate from a mildly basic dopamine·HCl solution. To visualize the thickness of the pDA coating we took advantage of the high affinity of polydopamine coatings for metals[30] and "stained" the polydopamine coating by immersion in a dilute silver salt solution, whereupon silver ions were bound to the polydopamine coating and provided image contrast for determination of the coating thickness. SEM analysis of a fracture surface of a silver-stained pDA coated substrate indicated that the thickness of the pDA coating was approximately 4 nm (Figure 2).

pDA substrates were then used as a starting point to fabricate three additional types of coatings. The first coating consisted of grafted PEG on polydopamine-coated PC (PEG substrate), generated by exploiting the reactivity of the terminal sulfhydryl group of mPEG-SH toward quinones within the polydopamine coating. A second coating contained silver nanoparticles deposited

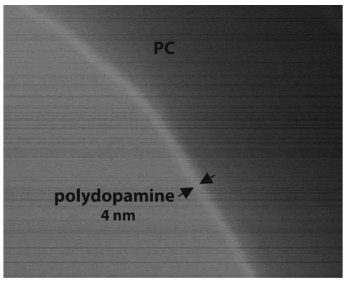

Figure 2. Immersion of PC substrate in alkaline dopamine·HCl results in deposition of a uniform 4 nm thick polydopamine coating. The figure shows a profile of a fractured pDA substrate imaged by SEM using a combination of secondary electron and backscattered electron detectors. The polydopamine coating was revealed by immersion in 1 mM $AgNO_3$ solution for 2 h and then fractured prior to imaging. Silver was used in this experiment as a "stain" to reveal the polydopamine coating without forming silver nanoparticles (Supporting Information, Figure S3).

onto polydopamine (Ag substrate), accomplished by immersion of pDA substrate in an aqueous silver nitrate solution. The silver-coating protocol was identified via a Design of Experiment approach, which deduced that silver nanoparticle formation was most influenced by silver nitrate concentration and incubation time (see the Supporting Information, Figure S2). Finally, a dual antifouling/antimicrobial coating (Ag+PEG) was created by recoating Ag substrates with polydopamine followed by grafting PEG brushes as described. An intermediate polydopamine layer was necessary, as direct conjugation of mPEG-SH to Ag substrates resulted in delamination of the silver layer, perhaps because of the high reactivity of mPEG-SH to metalized silver under cloud point conditions.

For comparison purposes, we also prepared silver containing PC substrates using a method similar to that used to fabricate commercially available silver coatings (DDS substrate). The DDS substrate was further coated with polydopamine (DDS+pDA substrate) and subsequently conjugated with mPEG-SH to render DDS a dual antifouling/antimicrobial surface (DDS+pDA+PEG substrate).

X-ray photoelectron spectroscopy was employed to confirm each modification step (Figure 3A,B). Polydopamine deposition was reflected by the presence of the N_{1s} (399 eV) peak in addition to the C_{1s} (284.7 eV) and O_{1s} (531 eV) peaks present in bare polycarbonate. S_{2p} (162.6 eV) peaks, as well as a C_{1s} peak at 286.7 eV, indicating C−O bonds, emerged on substrates subsequently treated with mPEG-SH (PEG and Ag+PEG). Several peaks corresponding to silver emerged in silver treated substrates, most prominently the Ag_{3d} (368.1−374 eV) peaks. They were still visible in the Ag+PEG substrate − however, at reduced amplitude due to the overlaying PEG brush. The presence of silver nanoparticles on DDS was verified by the presence of Ag_{3d} peaks, whose intensity similarly reduced after subsequent polydopamine coating and PEG grafting. Incubation of bare PC or DDS with mPEG-SH or silver nitrate solution did not result in significant XPS spectral changes, indicating the necessity of polydopamine for the modifications (data not shown). Static contact angle measurements (Figure 3C) were performed on unmodified and modified surfaces, revealing a decrease of approximately 25° between untreated and modified substrates.

We characterized the surface morphology of polydopamine-mediated antibacterial substrates using atomic force microscopy (AFM) and scanning electron microscopy (SEM). Treatment of

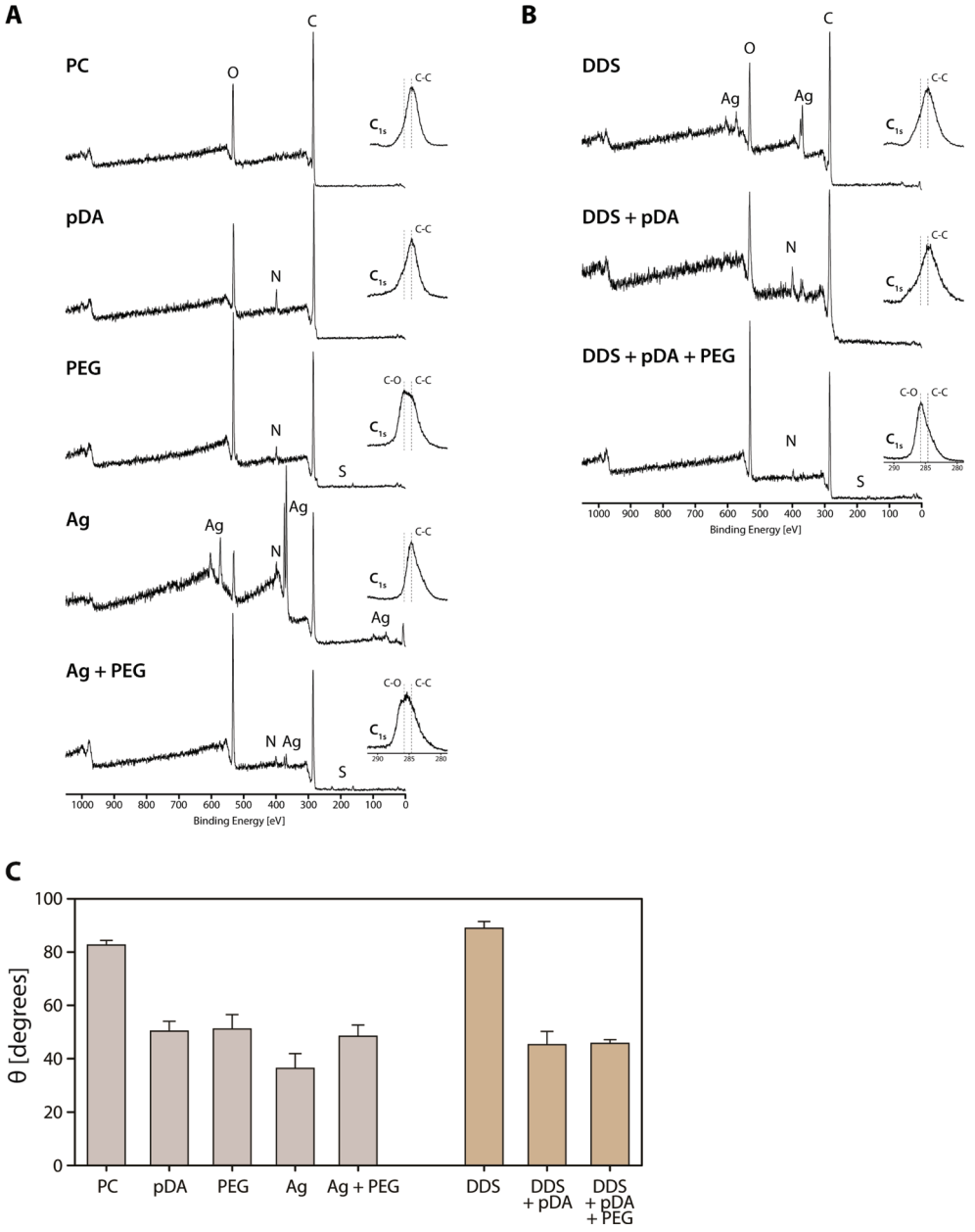

Figure 3. X-ray photoelectron spectroscopic and contact angle analysis of modified surfaces. XPS survey scans of (A) PC, pDA, PEG, Ag, Ag+PEG substrates and (B) DDS, DDS+pDA, DDS+pDA+PEG substrates. Presence of peaks is annotated with the corresponding label for the atom. C_{1s} detail scans are provided as insets with dotted lines indicating 286.7 and 284.7 eV for C−O and C−C C_{1s} peaks, respectively. (C) Static contact angles on modified substrates using water as liquid phase ($N = 3$).

PC substrates with polydopamine resulted in a minor increase in surface roughness, and further PEGylation resulted in a cloudlike surface morphology, which has previously been reported for grafted PEG brushes (Figure 4A).[40] DDS substrates, on the other hand, displayed profound differences in surface roughness in comparison to PC, presumably due to discontinuous silver nanoparticle deposition (Figure 4B). However, further treatment of DDS substrates with polydopamine deposition and subsequent PEG grafting did not visibly increase the surface roughness.

Images of Ag and Ag+PEG substrates demonstrated the presence of surface bound silver nanoparticles (Figure 5A). For Ag substrates prepared following our standard protocol, the nanoparticle sizes ranged from roughly 12−48 nm in diameter and were binomially distributed, with distributions centered on ∼26 nm and ∼38 nm (Figure 5B). EDS analysis confirmed that the nanoparticles observed in AFM and SEM images were composed of silver and that regions without nanoparticles had no detectable level of silver (Figures 6A,B). UV−vis analysis further confirmed the formation of silver nanoparticles through emergence of a silver plasmon resonance, evident by an increase in absorbance between 420 to 450 nm (Figure 6C). The number and size of the particles could be tailored via variation of incubation time with dopamine·HCl, silver nitrate concentration and incubation time (see the Supporting Information, Figure S2). The origin of the binomial distribution is uncertain, although one possible explanation is

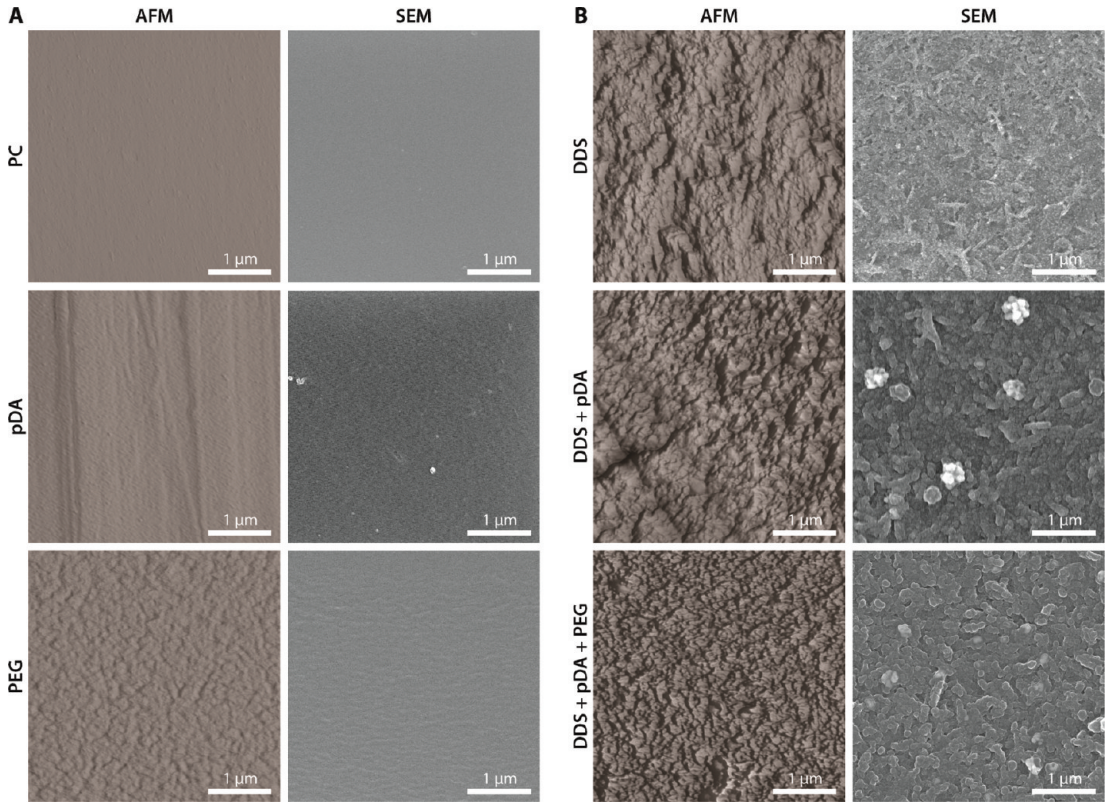

Figure 4. Nanoscale imaging of polydopamine coated surfaces. 3D-rendered 5 × 5 μm^2 AFM images (left) and SEM images (right) of (A) PC, pDA, PEG and (B) DDS, DDS+pDA and DDS+pDA+PEG surfaces.

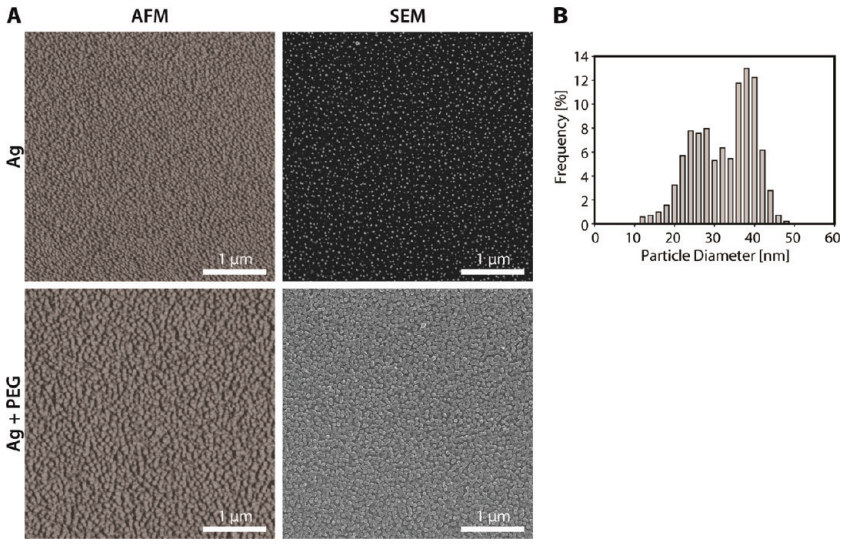

Figure 5. AFM and SEM analysis of silver nanoparticle deposition on polydopamine. (A) 3D-rendered 5 × 5 μm AFM images (left) and SEM images (right) of Ag and Ag+PEG surfaces. (B) Histogram of individual nanoparticle diameters obtained from SEM images of the Ag substrate. (N = 3 images and N = 5628 particles).

that Ostwald ripening occurs during nanoparticle growth, as it is energetically more favorable for small particles to fuse instead of growing independently of each other.[41] With increasing incubation times, a higher percentage of larger particles could form because of continued fusion of smaller particles.

Polydopamine-Based Coatings Allow Long-Term Silver Release. To determine whether polydopamine-based silver coatings release silver, we measured time-dependent silver release from Ag and Ag+PEG substrates into saline. ICP-MS measurements revealed roughly constant silver release into solution during the first 6 days for silver containing polydopamine (Ag) (Figure 7A), after which little additional silver release was observed. Addition of PEG reduced the rate of silver release by 70% but extended the release time to at least 10 days, indicating

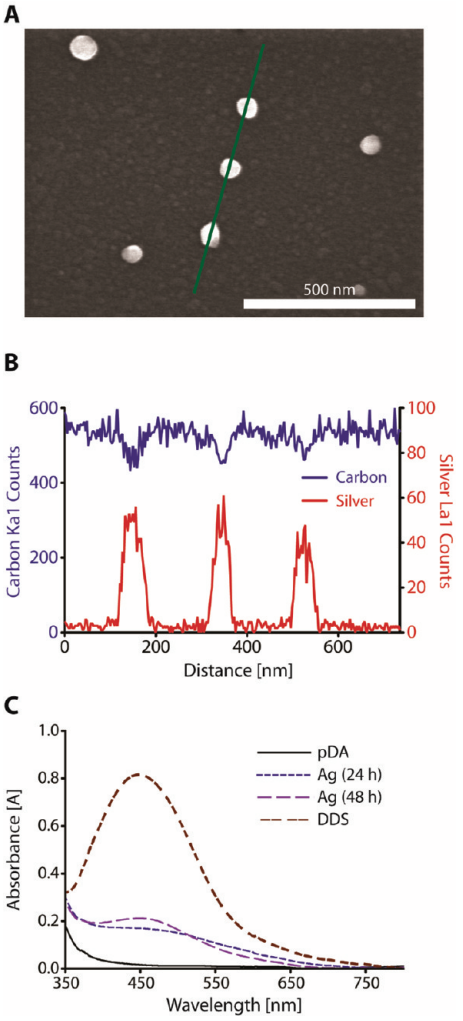

Figure 6. Nanoparticles are composed of silver. (A) SEM image of individual nanoparticles in Ag surfaces. (B) EDS line scans for carbon and silver along the line drawn over 3 nanoparticles. (C) UV−vis spectra of silver-containing surfaces. PC spectrum was not significantly different from pDA and is not shown.

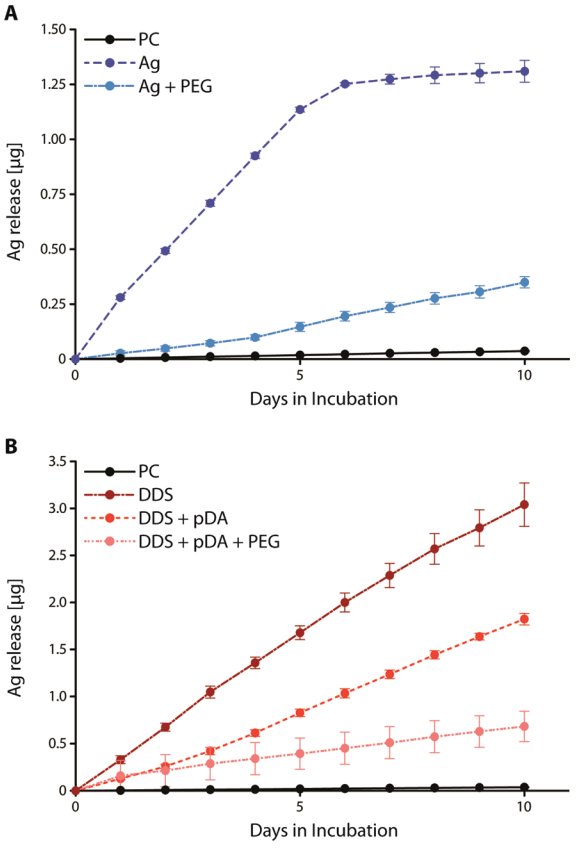

Figure 7. Silver release from Ag and Ag+PEG surfaces is sustained for nearly a week, and can be prolonged via an additional layer of pDA and PEG. Cumulative silver mass released into 5 mL saline solutions containing (A) Ag or Ag+PEG surfaces or (B) modified DDS surfaces. Solutions were changed every 24 h and silver concentration measured via ICP-MS.

coverage of silver by PEG could provide value in modulation of silver release as diffusion barriers. DDS substrates displayed approximately twice the total silver release compared to Ag substrates, which was lowered by 40 and 60% with subsequent coating with polydopamine and PEG, respectively (Figure 7B).

Polydopamine-Based Coatings Display Antifouling and Antimicrobial Behavior. We probed the antifouling and antimicrobial performance of the polydopamine-enabled coatings with two different assays. Antifouling was assessed via an attachment assay, in which cells were seeded in saline solution and allowed to attach for 24 h before washing away unattached cells and imaging cells remaining on the surface (Figure 8A and Figure S4 in the Supporting Information). Antimicrobial performance was assessed by a cell death assay, where cells were prestained with a live/dead stain and exposed to the surface for 24 h before imaging to determine live/dead cell coverage (Figure 8B). The antifouling assay therefore simply measures the ability of cells to attach to the substrate and does not discriminate between live and dead cells, whereas the antibacterial assay measures the efficiency of killing but does not discriminate between attached and unattached cells. Two gram negative strains, *E. coli* and *P. aeruginosa*, and one gram positive strain, *S. epidermidis*, were used to demonstrate broad antibacterial properties of the substrate coatings.

Unmodified PC supported attachment of all three bacterial strains (Figure 8A and Figure S2 in the Supporting Information), and coating of PC with polydopamine had no effect or led to a modest increase in bacterial attachment. This result was not unexpected, as polydopamine has been previously shown to support cell attachment.[30] Substrates containing silver alone (Ag and DDS) also supported bacterial attachment at levels equal to or higher than PC controls, and further deposition of pDA onto these silver containing substrates did not improve attachment resistance. In the case of *S. epidermidis* in particular, attachment on Ag substrates significantly increased over PC controls, which we speculate could be attributed to the increased surface roughness of the silver-modified substrates. Likewise, because of its greater surface roughness, DDS substrates demonstrated even greater fouling than Ag substrates for *S. epidermidis* and *P. aeruginosa*.

The most striking feature of the attachment assay was observed upon conjugation of PEG onto pDA, Ag and DDS+pDA substrates, which abrogated attachment of all three bacterial strains tested. This is likely due to the steric hindrance of PEG brushes toward bacterial cell attachment, a physical effect unrelated to the presence of active antibacterial agents. A reduction

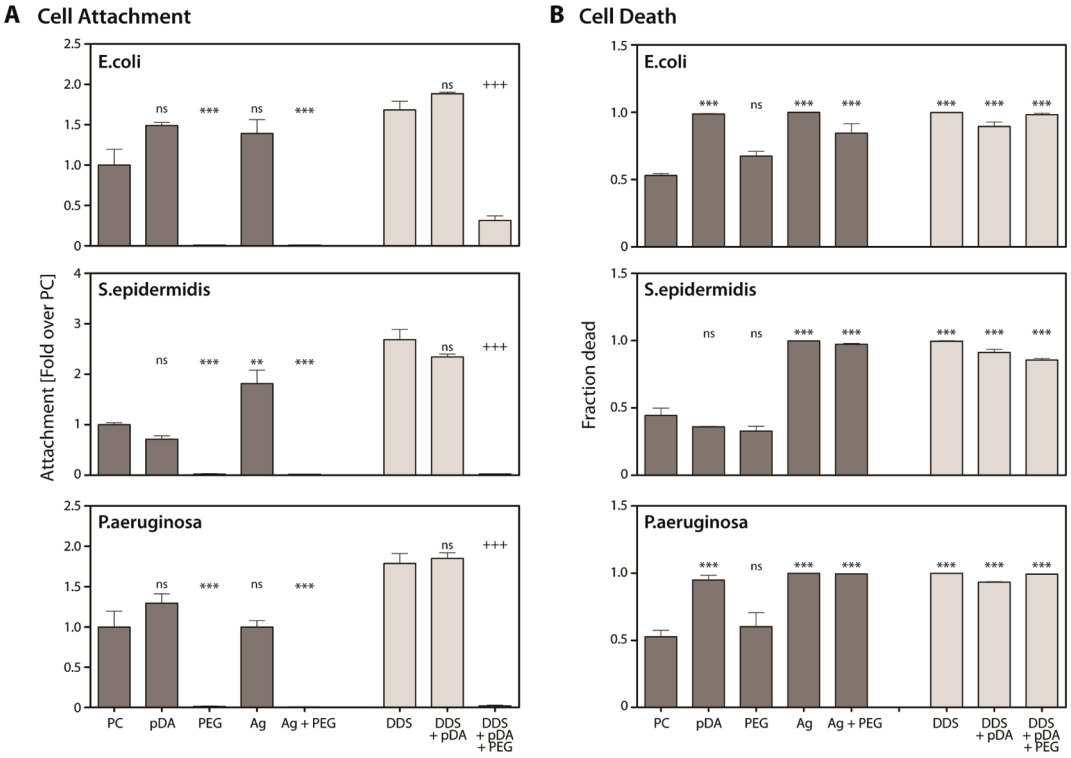

Figure 8. Silver deposition via polydopamine followed by PEGylation prevents attachment and results in cell death, respectively, for a variety of gram-positive and −negative bacterial strains. (A) Normalized attachment of E.coli, S.epidermidis, or P.aeruginosa on polydopamine-modified substrates. 1×10^8 CFU/mL of each strain in saline was seeded onto the surfaces for 24 h before washing and staining with a live/dead stain. Fluorescent images were taken and analyzed for total % area coverage of both live and dead cells. All values were normalized to % coverage on PC control. (B) Fraction cell death of E.coli, S.epidermidis, or P.aeruginosa on polydopamine-modified surfaces. Twenty microliters of 2.5×10^9 CFU/mL of each strain in saline preincubated with the live/dead stain was seeded on a glass slide and the substrate was placed on top of cells. Cells were sealed from the outside. Cells were imaged after 24 h of incubation, and % area covered by dead cells over total % area covered by both live and dead cells was evaluated. All values were normalized to PC control. Representative images are included in the Supporting Information, Figures S4 and S5. Statistical significance was evaluated via one-way ANOVA and the Bonferroni post-test. ** $p < 0.01$, *** $p \ll 0.001$ compared to PC control. +++ $p \ll 0.001$ compared to DDS control. ns = not significant. $N = 3$ biological replicates.

in the overall surface energy of the substrate following PEGylation may also be contributing to the observed decrease in attachment.

Ag, Ag+PEG, and all DDS substrates displayed antimicrobial effects per our death assay (Figure 8B and Figure S5 in the Supporting Information). After a 24 h incubation time, almost all of the cells were found to be dead on all silver-loaded substrates, with a slightly lesser fraction observed for Ag+PEG substrates for *E. coli*. As expected, PEG substrates did not give rise to an observable increase in bacterial killing because of a lack of an active antibacterial component. Interestingly, pDA substrates exhibited antimicrobial behavior against *E. coli* and *P. aeruginosa* after 24 h of incubation. We observed that the pH of saline solution in contact with pDA substrates became acidic (see the Supporting Information, Figure S6), and that this may adversely affect bacterial viability. A subsequent comparison of bacterial cell viability on pDA substrates in phosphorus-buffered saline (PBS) at pH 7.4 versus unbuffered saline indeed showed that incubation in PBS did not result in cell death on pDA substrates, whereas cells on Ag substrates displayed high cell death (see the Supporting Information, Figures S7 and S8). This result demonstrates that the killing effect of *E. coli* and *P. aeruginosa* arises from silver, not polydopamine. The lack of antimicrobial effect of pDA substrates on *S. epidermidis* in saline might be explained by the inherent difference in responses to environmental pH changes by gram negative and gram positive bacteria. Gram negative bacteria, such as *E. coli* and *P. aeruginosa*, attempt to maintain a constant intracellular pH through active transport of ions, while gram positive bacteria, such as *S. epidermidis*, preserve a constant pH gradient across the cellular membrane. Maintaining a steady intracellular pH becomes substantially more difficult as the environmental pH moves toward either extreme.[42,43]

If we consider the results of both assays together, it is clear that silver containing substrates are effective at killing bacteria but not at preventing their attachment. The combination of attachment prevention and bacterial death was only observed for substrates that combined silver and PEG. In other words, the combination of PEG and silver provides both "on-surface" and "off-surface" effects. In this respect, polydopamine serves an important role in facilitating both silver and PEG deposition onto the substrate using simple protocols. For existing silver-based coatings such as DDS, polydopamine allows for coating of the substrate with antifouling polymer while still preserving the antibacterial effect of silver.

CONCLUSIONS

We demonstrated a novel and simple immersion strategy for substrate coatings that inhibit bacterial attachment and actively kill bacteria through silver release. The strategy is enabled by a polydopamine "primer," onto which antifouling polymer is

grafted and into which silver nanoparticles are nucleated from a silver salt solution. Surface characterization techniques verified the successful and efficient grafting of PEG and silver onto polydopamine. Release of silver over clinically relevant periods was confirmed using ICP-MS, which can be modulated by creating additional diffusion barriers. Finally, we confirmed the antifouling and antimicrobial performance of the novel surfaces against both gram-positive and gram-negative bacterial strains. Resistance to bacterial attachment was correlated with the presence of grafted PEG, whereas bacterial killing was afforded by silver encapsulated within the polydopamine underlayer. Thus, our approach represents a simple method to incorporate both passive (antifouling) and active (antimicrobial) entities into a surface coating. The ability of polydopamine coatings to be applied to many different materials, combined with its chemical versatility in reacting with a variety of polymers, biomolecules, ions, and other compounds, suggests significant potential for expansion of this concept to other coatings in the future.

■ ASSOCIATED CONTENT

Supporting Information. Cloud point determination and silver nanoparticle loading optimization data for mPEG-SH and silver surface modifications; composite fluorescence images from bacterial attachment and viability assays, along with data for antimicrobial activity of pDA and Ag surfaces in buffered media. This material is available free of charge via the Internet at http://pubs.acs.org/.

■ AUTHOR INFORMATION

Corresponding Author

*Address: Biomedical Engineering Department, Northwestern University, 2145 Sheridan Road, Evanston, IL 60208. Phone (847)467-5273. Fax (847)491-4928. E-mail: philm@northwestern.edu.

Author Contributions

‡These authors contributed equally to this work.

■ ACKNOWLEDGMENT

We thank Dr. John-Bruce Green for productive discussions. This work was supported by Baxter Healthcare.

■ REFERENCES

(1) Klevens, R. M.; Edwards, J. R.; Richards, C. L.; Horan, T. C.; Gaynes, R. P.; Pollock, D. A.; Cardo, D. M. *Public Health Rep.* **2007**, *122*, 160–166.

(2) Johnson, J. R.; Kuskowski, M. A.; Wilt, T. J. *Ann. Intern. Med.* **2006**, *144*, 116–126.

(3) Pierce, G. E. *J. Ind. Microbiol. Biotechnol.* **2005**, *32*, 309–318.

(4) Donlan, R. M. *Emerging Infect. Dis.* **2001**, *7*, 277–281.

(5) Denstedt, J. D.; Cadieux, P. A. *Curr. Opin. Urol.* **2009**, *19*, 205–210.

(6) Donlan, R. M.; Costerton, J. W. *Clin. Microbiol. Rev.* **2002**, *15*, 167–193.

(7) Costerton, J. W.; Stewart, P. S.; Greenberg, E. P. *Science* **1999**, *284*, 1318–1322.

(8) Krishnan, S.; Weinman, C. J.; Ober, C. K. *J. Mater. Chem.* **2008**, *18*, 3405–3413.

(9) Banerjee, I.; Pangule, R. C.; Kane, R. S. *Adv. Mater.* **2011**, *23*, 690–718.

(10) Kim, J. S.; Kuk, E.; Yu, K. N.; Kim, J. H.; Park, S. J.; Lee, H. J.; Kim, S. H.; Park, Y. K.; Park, Y. H.; Hwang, C. Y.; Kim, Y. K.; Lee, Y. S.; Jeong, D. H.; Cho, M. H. *Nanomed. Nanotechnol. Biol. Med.* **2007**, *3*, 95–101.

(11) Lok, C. N.; Ho, C. M.; Chen, R.; He, Q. Y.; Yu, W. Y.; Sun, H.; Tam, P. K. H.; Chiu, J. F.; Che, C. M. *J. Biol. Inorg. Chem.* **2007**, *12*, 527–534.

(12) Ye, S. J.; Majumdar, P.; Chisholm, B.; Stafslien, S.; Chen, Z. *Langmuir* **2010**, *26*, 16455–16462.

(13) Tiller, J. C.; Liao, C. J.; Lewis, K.; Klibanov, A. M. *Proc. Natl. Acad. Sci. U. S. A.* **2001**, *98*, 5981–5985.

(14) Maneerung, T.; Tokura, S.; Rujiravanit, R. *Carbohydr. Polym.* **2008**, *72*, 43–51.

(15) Rai, M.; Yadav, A.; Gade, A. *Biotechnol. Adv.* **2009**, *27*, 76–83.

(16) Monteiro, D. R.; Gorup, L. F.; Silva, S.; Negri, M.; de Camargo, E. R.; Oliveira, R.; Barbosa, D. B.; Henriques, M. *Biofouling* **2011**, *27*, 711–719.

(17) Zhu, X.; Tang, L.; Wee, K.-H.; Zhao, Y.-H.; Bai, R. *Biofouling* **2011**, *27*, 773–786.

(18) Yasuyuki, M.; Kunihiro, K.; Kurissery, S.; Kanavillil, N.; Sato, Y.; Kikuchi, Y. *Biofouling* **2010**, *26*, 851–8.

(19) Roe, D.; Karandikar, B.; Bonn-Savage, N.; Gibbins, B.; Roullet, J. B. *J. Antimicrob. Chemother.* **2008**, *61*, 869–876.

(20) Park, K. D.; Kim, Y. S.; Han, D. K.; Kim, Y. H.; Lee, E. H. B.; Suh, H.; Choi, K. S. *Biomaterials* **1998**, *19*, 851–859.

(21) Fernandez, I. C. S.; van der Mei, H. C.; Lochhead, M. J.; Grainger, D. W.; Busscher, H. J. *Biomaterials* **2007**, *28*, 4105–4112.

(22) Efremova, N. V.; Sheth, S. R.; Leckband, D. E. *Langmuir* **2001**, *17*, 7628–7636.

(23) Dalsin, J. L.; Hu, B. H.; Lee, B. P.; Messersmith, P. B. *J. Am. Chem. Soc.* **2003**, *125*, 4253–4258.

(24) Fan, X. W.; Lin, L. J.; Messersmith, P. B. *Biomacromolecules* **2006**, *7*, 2443–2448.

(25) Nejadnik, M. R.; van der Mei, H. C.; Norde, W.; Busscher, H. J. *Biomaterials* **2008**, *29*, 4117–4121.

(26) Glinel, K.; Jonas, A. M.; Jouenne, T.; Leprince, J.; Galas, L.; Huck, W. T. S. *Bioconjugate Chem.* **2009**, *20*, 71–77.

(27) Statz, A. R.; Park, J. P.; Chongsiriwatana, N. P.; Barron, A. E.; Messersmith, P. B. *Biofouling* **2008**, *24*, 439–448.

(28) Ho, C. H.; Tobis, J.; Sprich, C.; Thomann, R.; Tiller, J. C. *Adv. Mater.* **2004**, *16*, 957–961.

(29) Sousa, C.; Henriques, M.; Oliveira, R. *Biofouling* **2011**, *27*, 609–20.

(30) Lee, H.; Dellatore, S. M.; Miller, W. M.; Messersmith, P. B. *Science* **2007**, *318*, 426–430.

(31) Waite, J. H.; Tanzer, M. L. *Science* **1981**, *212*, 1038–1040.

(32) Waite, J. H. *Integr. Comp. Biol.* **2002**, *42*, 1172–1180.

(33) Lee, H.; Scherer, N. F.; Messersmith, P. B. *Proc. Natl. Acad. Sci. U.S.A.* **2006**, *103*, 12999–13003.

(34) Lee, Y. H.; Lee, H.; Kim, Y. B.; Kim, J. Y.; Hyeon, T.; Park, H.; Messersmith, P. B.; Park, T. G. *Adv. Mater.* **2008**, *20*, 4154–4157.

(35) McCann, M. T.; Gilmore, B. F.; Gorman, S. P. *J. Pharm. Pharmacol.* **2008**, *60*, 1551–1571.

(36) Sharma, S.; Johnson, R. W.; Desai, T. A. *Biosens. Bioelectron.* **2004**, *20*, 227–239.

(37) Lee, H.; Lee, Y.; Statz, A. R.; Rho, J.; Park, T. G.; Messersmith, P. B. *Adv. Mater.* **2008**, *20*, 1619–1623.

(38) Ham, H. O.; Liu, Z. Q.; Lau, K. H. A.; Lee, H.; Messersmith, P. B. *Angew. Chem., Int. Ed.* **2011**, *50*, 732–736.

(39) Lee, H.; Rho, J.; Messersmith, P. B. *Adv. Mater.* **2009**, *21*, 431–434.

(40) Li, J.; Tan, D.; Zhang, X.; Tan, H.; Ding, M.; Wan, C.; Fu, Q. *Colloids Surf., B* **2010**, *78*, 343–50.

(41) Voorhees, P. W. *J. Stat. Phys.* **1985**, *38*, 231–252.

(42) Arthur, L. K. *Bact. Growth Form.* 2001; pp 396−400.

(43) Storz, G.; Hengge-Aronis, R. *Bact. Stress Responses* 2000; pp 99−101.